**Supplementary Material**

**DETAILED METHODS**

*Cell models.* Studies were performed in human Mz-Cha-1 cells (1) and in mouse small and large cholangiocytes isolated from normal mice (BALB/c) and immortalized by transfection with the SV40 large-T antigen gene as previously described (2, 3). Both cell types exhibit phenotypic features of differentiated biliary epithelium(1, 4) and have been utilized as models for biliary ATP release, signaling, and secretion(5-9). Cells were maintained in culture as described (2, 3). For studies of apical surface liquid (ASL), MLC cells were cultured on collagen-coated semi-permeable (24 mm diameter, 0.4 mm pore) transwell supports (Costar Corning, Acton, MA) 7-10 days before ASL studies. This protocol permits highly polarized cells and the development of a high transepithelial resistance ($R_t$ > 1,000 Wcm$^2$) (10, 11).

*Perfusion system*: Shear was applied to cells in a parallel plate chamber (24 x 13 x 4.1 mm, RC-25F, Warner Instruments, Hamden, CT) as described(12) . Flow was applied by a dual syringe pump (Pump 33, Harvard apparatus, Holliston, MA). The equation relating shear stress to volumetric flow rate through the chambers is given by $t_w$= 6mQ/a$^2$b, where mis the viscosity of the solution (poise), Q=flow rate (ml/sec), a=chamber height (cm), b=chamber width (cm).

*Measurement of $Na^+$ currents.* Membrane $Na^+$ currents were measured using whole-cell patch clamp techniques as previously reported (13). Cells on a cover slip were

mounted in a chamber (volume ~400 ml) and whole cell currents measured with low $Cl^-$ solutions to minimize the contribution of flow-stimulated $Cl^-$ currents (14). The extracellular solution contained (in mM): 145 NaGlu, 1 $CaCl_2$, 1 $MgCl_2$, 10 glucose, and 10 HEPES/NaOH (pH ~7.40; 300mOsm). The intracellular (pipette) solution for whole cell recordings contained (in mM): 145 NMDGGLu, 2 $MgCl_2$, 2 Na2ATP, 10 HEPES/Tris, (pH 7.3; 290 mOsm). In select studies, $Na^+$ was replaced with NMDG. Patch pipettes were pulled from Corning 7052 glass and had a resistance of 6-12 MW. Recordings were made with an Axopatch ID amplifier (Axon Instruments, Foster City, CA), and were digitized (1 kHz) for storage on a computer and analyzed using pCLAMP version 10.0 programs (Axon Instruments, Burlingame, CA) as previously described (11, 14). Two voltage protocols were utilized: 1) holding potential –40 mV, steps to -100 mV and 0mv and +100mv at 5 second intervals (for real-time tracings), 2) holding potential –40 mV, with 400 ms steps from –100 mV to +100 mV in 10 mV increments. Current-voltage (I-V) relations were generated from the “step” protocols as indicated. Pipette voltages (Vp) are referred to the bath. In the whole-cell configuration, Vp corresponds to the membrane potential, and upward deflections of the current trace indicate outward membrane current. A dose-response curve with variable Hill slope according to the equation: $y = A1 + (A2-A1)/1+10^{(\log x0-x)p}$ was used to plot changes in shear versus the magnitude of current response where y = current density (pA/pF), x = shear (dyne/$cm^2$), A1 = minimum, A2 = maximum, and p is the Hill slope. Results are compared with control studies measured on the same day to minimize any effects of day-to-day variability and reported as current density (pA/pF) to normalize for differences in cell size.

*Measurement of Apical Surface Liquid (ASL) height.* The height of the fluid level at the apical membrane of confluent mouse cholangiocyte monolayers was performed according to a modified technique previously described in airway epithelial monolayers(15) . Briefly, confluent MLC cells on 24mm collagen-coated transwell permeable membranes (Corning # 3491) with a transepithelial resistance > 1,000 $\Omega cm^2$ were washed with PBS and labeled with Calcein-AM at a concentration of 3 mM for 20 minutes in a 37°C $CO_2$ incubator. The transwell was then placed on the surface of a glass-bottomed MatTek 35mm dish (MatTek Corp, Ashland, MA) over a serosal reservoir (80 ml PBS) and 80 ml of Dextran-Red (10 kDa, 2 mg/ml, Molecular Probes) in PBS was added to the apical chamber. To prevent evaporation of the Dextran-Red, 400 ml of Fluorinert FC-770 was carefully added to the surface of the transwell. Transwells were then mounted on a Zeiss LSM510 Confocal microscope and images acquired with the Zeiss AIM software (Carl Zeiss Microimaging, Inc. Thornwood, NY). Each sample was imaged at 5 different locations (center and 4 circumferential quadrants). The Zeiss AIM software has the capability to capture images using a line scan method and allows z-stacking of the line scan images to generate a cross-sectional view of the sample. Images were acquired using a Zeiss 40x/0.8 water immersion lens at 5 mm intervals giving us a resolution of 2.276 mm per pixel. All images were acquired at the same electronic gain, offset, and laser powers and analyzed with ImageJ (http://rsb.info.nih.gov), as previously described(15, 16).

*Detection of ENaC.* PCR products representing the a, b, and g subunits of ENaC were detected utilizing specific primers (Supplemental Table 1) and oligo(dt) primer and

Superscript RNase H-reverse transcriptase (Invitrogen, Carlsbad, CA). The reaction mixtures (25 μl) contained 2 μl of cDNA, 1 μl of dNTP (10 mmol/L), 2.5 μl of 10Xbuffer, 1.5 μl of $MgCl_2$ (25 mmol/L), 2.5 U Taq Polymerase (Invitrogen, Carlsbad, CA) and 50 pmol of each primer. The mixture was subjected to 30 cycles of amplification (94°C for 60 s; denaturation, 60°C for 60 s annealing and 72°C for 60 s extension). Quantitative assessment was determined by real-time PCR using ABI Prism 7900HT Sequence detection System (Applied Biosystems, Life Technologies, Carlsbad, CA). Amplification reactions were performed in a final volume of 10 μl containing cDNA from 10 ng of reverse transcribed total RNA, 150 nM each of forward and reverse primers (Supplemental Table 2) and TaqMan Universal Master MixII with UNG (Applied Biosystems). ENaCa protein was detected by Western blot utilizing primary anti-human ENaCα, which recognizes an extracellular region contained in both the full-length and cleaved protein,1:200 (Alomone labs, Israel), followed by incubation with peroxidase-conjugated goat anti-rabbit antibody, dilution 1:10,000 (Jackson ImmunoResearch Laboratories, Inc., PA), and visualized by the $ECL^+$ detection kit (GE Healthcare) and band intensity quantified using standard software (GeneTool, Syngene).

*Immunofluorescence*. Localization of ENaCa protein was performed in confluent MLC monolayers. MLC on collagen coated tissue culture chamber slides (BD BioCoat) were fixed in 25% acetic acid/75% ethanol (v/v) for 10 min or 4% paraformaldehyde permeabilized with 1% triton-X 100 for 10 min, incubated with 5% normal donkey serum, and then incubated overnight at 4°C with anti-ENaCa antibody (Alomone labs #ASC-030) and then Dylight 488 conjugated donkey anti-rabbit (Jackson

Immunoresearch, 1:600) and counter-labeled with Alexa Fluor 555 phalloidin. Control cells were prepared by omitting either primary or secondary antibodies from the incubation solution. The slides were coverslipped with Mowiol Æ 4-88 with 2.5% DABCO and left overnight in the dark at R.T. The slides were imaged using the Leica TCS SP5 confocal microscope (Leica Micro-systems, CMS GMBH) with custom software (Leica Micro-systems LAS AF).

*Immunohistochemistry.* Immunohistochemistry was performed on paraffin sections of mouse liver to evaluate localization of ENaCa. Wild-type C57BL/6 mouse liver sections were fixed in10% neutral buffered formalin and paraffin embedded. Four micron thick sections were mounted on positively charged glass slides and baked at 65°C for 45 minutes. All further processing steps were performed on the Dako Omnis automated immunohistochemistry platform (Glostrup, Denmark). Deparaffinization was followed by heat and low pH Tris antigen retrieval. Sections were incubated with mouse polyclonal ENaCa antibody at a 1:800 dilution (#PA1-920A, Thermo Fisher Scientific, Waltham, MA). Endogenous peroxidase blocking was performed and then followed by incubation with a secondary HRP antibody mixture of goat anti-rabbit and goat anti-mouse for 20 minutes. Chromogenic precipitate was generated using a combination of DAB and Dako Omnis substrate buffer for 5 minutes. Sections were counterstained with hematoxylin.

*Overexpression of ENaC subunits.* Full-length ENaC α, β, γ, channel subunits were kind gift from Chou-long Huang (UT Southwestern) (17) and were amplified and purified by using Macherey-Nagel NucleoBond® Xtra Midi / Maxi. Cells grown to ~70% confluency in 35 mm dishes were treated with 4µg of total plasmid cDNA encoding α, β, γ ENaC

and GFP using the lipofectamin 2000 (Invitrogen) per the manufacturer's recommendations. GFP-labeled cells were used for patch clamp analysis or extracted for protein analysis 48 hours after transfection.

*ENaC silencing.* ENaCα was suppressed by specific ENaCα siRNA (NM_001159576). siRNAs were designed and synthesized by IDT (5'- AGC UUU GAC AAG GAA CUU UCC UAA G -3'; 3'-CCU CGA AAC UGU UCC UUG AAA GGA UUC-5') and control sequence (5'-CGU UAA UCG CGU AUA AUA CGC GUA T -3', 3'-AUA CGC GUA UUA UAC GCG AUU AAC GAC -5'). Control and siRNA (20nM) were transfected in Mz-Cha-1 cell by using Lipofectamine RNAiMAX reagent from Invitrogen. Block-it$^{TM}$ Fluorescent Oligo (catalog No. 2013, Invitrogen) was used to optimize transfection conditions and for selection of transfected cells for whole-cell patch clamp current recording. Whole cell patch clamp experiments were done 48 hours after transfection.

*Reagents.* All reagents for Western blot were from Biorad. Trypsin was from Thermo Scientific (HyClone Laboratories, Inc.). All other reagents were obtained from Sigma-Aldrich (St. Louis, MO).

*Statistics.* Results are presented as the mean ± standard error, with *n* representing the number of culture plates or repetitions for each assay as indicated. Statistical analysis included Fisher's paired and unpaired t-test and ANOVA for multiple comparisons to assess statistical significance as indicated, and p values ≤ 0.05 were considered to be statistically significant.

**Supplemental Table 1**

**ENaC human**

**α primer**

Forward primer TAACTTGCGGCCTGGCGTGG.

Reverse primer GCTGGTCACGCTGCATGGCT.

**β primer**

Forward primer: ATGAGCTACCCCGGCGAGCA.

Reverse primer TGCGCTGAAGCTTGTCCACGA.

**γ primer**

Forward primer: GGAAGCGGAAAGTCGGCGGT.

Reverse primer: GCGTGAAATTCCTGGCATCACAGGA.

**ENaC Mouse**

**α primer**

Forward primer: GCACACCACCTCCGCCCAATC.

Reverse primer: CGCAGTGTCAGGGACAAACCATTGT.

β **primer**

Forward primer: CACACTGGAGCAGCTTCCTAAACA.

Reverse primer: TTGGAGTACTGGAAGGGGCTGGAA.

γ **primer**

Forward primer: ACACCTCGGAAACGCCGGGA.

Reverse primer: GAGTGAAGTTCCTGGCATCACAGG.

## Supplemental Material References

**Reference List**


1. **Knuth A, Gabbert H, Dippold W, Klein O, Sachsse W, Bitter-Suermann D, et al. Biliary Adenocarcinoma. Characterization of three new human tumor cell lines. J Hept 1985;1:579-596.**

2. **Francis H, Glaser S, Demorrow S, Gaudio E, Ueno Y, Venter J, et al. Small mouse cholangiocytes proliferate in response to H1 histamine receptor stimulation by activation of the IP3/CaMK I/CREB pathway. Am J Physiol Cell Physiol 2008 Aug;295(2):C499-C513.**

3. **Ueno Y, Alpini G, Yahagi K, Kanno N, Moritoki Y, Fukushima K, et al. Evaluation of differential gene expression by microarray analysis in small and large cholangiocytes isolated from normal mice. Liver Int 2003 Dec;23(6):449-459.**

4. **Basavappa S, Middleton JP, Mangel A, McGill J, Cohn JA, Fitz JG. Cl- and K+ transport in human biliary cell lines. Gastroenterology 1993;104:1796-1805.**

5. **Feranchak AP, Roman RM, Doctor RB, Salter KD, Toker A, Fitz JG. The lipid products of phosphoinositide 3-kinase contribute to regulation of cholangiocyte ATP and chloride transport. J Biol Chem 1999;274:30979-30986.**

6. **Feranchak AP, Doctor RB, Troetsch M, Brookman K, Johnson SM, Fitz JG. Calcium-dependent regulation of secretion in biliary epithelial cells: the role of apamin-sensitive SK channels. Gastroenterology 2004 Sep;127(3):903-913.**

7. **Roman RM, Wang Y, Fitz JG. Regulation of cell volume in a human biliary cell line: Calcium-dependent activation of K+ and Cl- currents. Am J Physiol 1996;271:G239-G248.**

8. **Roman RM, Feranchak AP, Salter KD, Wang Y, Fitz JG. Endogenous ATP regulates $Cl^-$ secretion in cultured human and rat biliary epithelial cells. Am J Physiol 1999;276:G1391-G1400.**

9. **Wang Y, Roman RM, Schlenker T, Hannun YA, Raymond JR, Fitz JG. Cytosolic calcium and protein kinase C(alpha) couple cellular metabolism to membrane K+ permeability in a human biliary cell line. J Clin Invest 1997;99:2890-2897.**

10. **Salter KD, Roman RM, LaRusso NR, Fitz JG, Doctor RB. Modified culture conditions enhance expression of differentiated phenotypic properties of normal rat cholangiocytes. Lab Invest 2000 Nov;80(11):1775-1778.**

11. **Schlenker T, Romac JMJ, Sharara A, Roman RM, Kim S, LaRusso N, et al. Regulation of biliary secretion through apical purinergic receptors in cultured rat cholangiocytes. Am J Physiol 1997;273:G1108-G1117.**

12. **Woo K, Dutta AK, Patel V, Kresge C, Feranchak AP. Fluid flow induces mechanosensitive ATP release, calcium signalling and Cl- transport in biliary epithelial cells through a PKCzeta-dependent pathway. J Physiol 2008 Jun 1;586(Pt 11):2779-2798.**

13. **Feranchak AP, Berl T, Capasso J, Wojtaszek PA, Han J, Fitz JG. p38 MAP kinase modulates liver cell volume through inhibition of membrane Na+ permeability. J Clin Invest 2001 Nov;108(10):1495-1504.**

14. **Dutta AK, Woo K, Khimji AK, Kresge C, Feranchak AP. Mechanosensitive Cl- secretion in biliary epithelium mediated through TMEM16A. Am J Physiol Gastrointest Liver Physiol 2013 Jan 1;304(1):G87-G98.**

15. **Tarran R, Button B, Boucher RC. Regulation of normal and cystic fibrosis airway surface liquid volume by phasic shear stress. Annu Rev Physiol 2006;68:543-561.**

16. **Tarran R, Trout L, Donaldson SH, Boucher RC. Soluble mediators, not cilia, determine airway surface liquid volume in normal and cystic fibrosis superficial airway epithelia. J Gen Physiol 2006 May;127(5):591-604.**

17. **Xu BE, Stippec S, Chu PY, Lazrak A, Li XJ, Lee BH, et al. WNK1 activates SGK1 to regulate the epithelial sodium channel. Proc Natl Acad Sci U S A 2005 Jul 19;102(29):10315-10320.**

*Supplemental Figure 1*

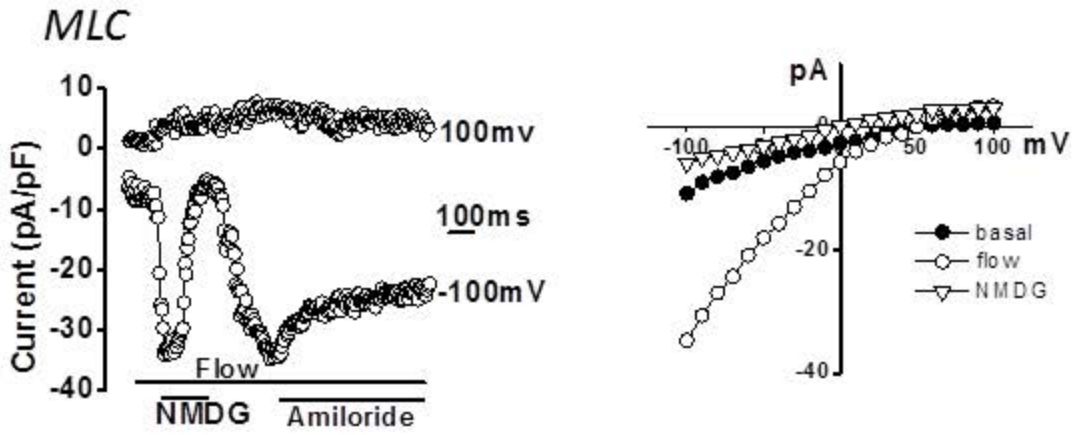

*Supplemental Figure 2*

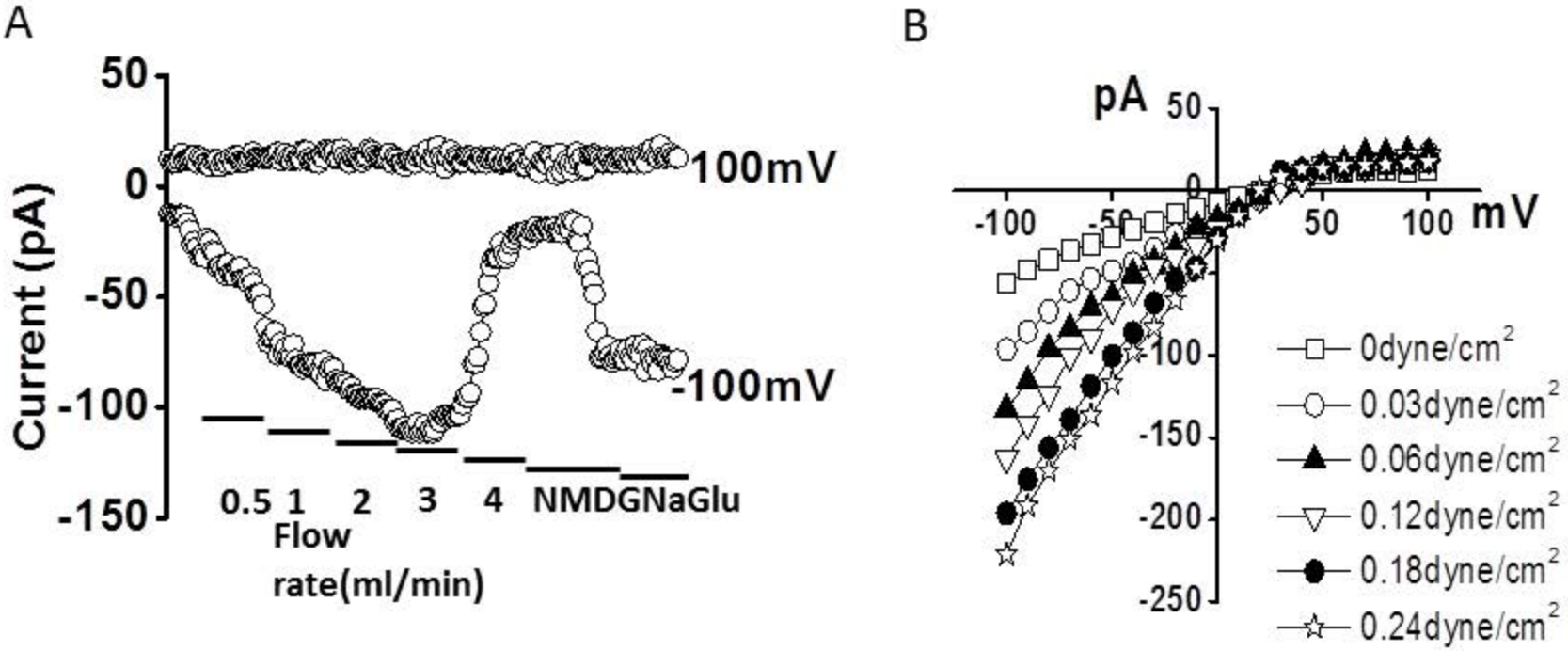

*Supplemental Figure 3*

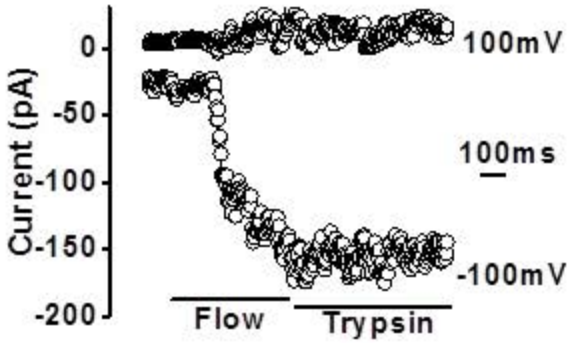


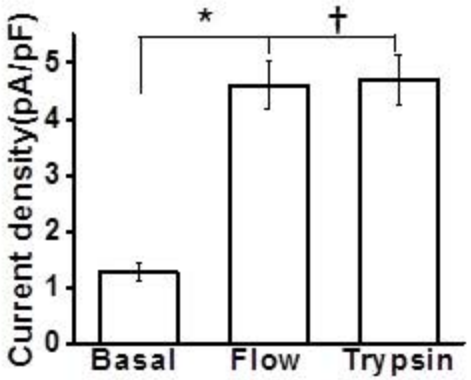

Supplemental Figure Legends

Supplemental Figure 1. Representative whole-cell recording of MLC cell. Whole-cell currents were measured during basal conditions and during exposure to flow of isotonic low $Cl^-$ extracellular buffer. Representative whole-cell recordings of MLC cell. Currents measured at −100 mV and at 100 mV are shown. Flow exposure (shear of 0. 24 dyne/$cm^2$) is indicated by the bar. Addition of amiloride (100 mM) or replacement of $Na^+$ with NMDG is indicated by the lower bars. The I–V plot shown in the right panel was generated from the voltage-step protocol (Methods) and currents during basal (-ÿ-) and flow-stimulated (**-o-**) conditions in the presence of amiloride (-D-) and with replacement of $Na^+$ with NMDG (-··-) are shown.

Supplemental Figure 2. The magnitude of flow-stimulated $Na^+$ currents is related to shear force. A. Representative whole-cell recording of Mz-Cha-1 cell. Currents measured at −100 mV and at +100 mV are shown. Graded increases in the flow rate are indicated by the bars. Currents were abolished with removal of $Na^+$ from the perfusate (NMDG) but rapidly activated again with $Na^+$ re-addition. B. I-V plot demonstrating an increase in inward currents with increasing shear and reversal potential at +40 mV.

Supplemental Figure 3. Modulation of $Na^+$ currents by proteases. Representative whole-cell recording of Mz-Cha-1 cell in the presence or absence of flow and trypsin. or trypsin inhibitor. Currents in response to flow (shear 0.24 dyne/$cm^2$) followed by

trypsin (top) and cumulative data demonstrating maximal current density measured at -100 mV during this sequential exposure (bottom). Bars represent Mean ± SEM; n=11 - 13 each, * $p<0.05$. There was no difference in the magnitude of current density between trypsin or flow, $^{\dagger}$p=n.s.